Journal of Colloid and Interface Science 644 (2023) 333–345

Contents lists available at ScienceDirect

Journal of Colloid And Interface Science

journal homepage: www.elsevier.com/locate/jcis

Effect of polymer architecture on the adsorption behaviour of amphiphilic copolymers: A theoretical study

Mingduo Mu [a,*], Frans A.M. Leermakers [b], Jianshe Chen [c], Melvin Holmes [a], Rammile Ettelaie [a,*]

[a] Food Colloids Group, School of Food Science and Nutrition, University of Leeds, Woodhouse Lane, Leeds LS2 9JT, UK
[b] Wageningen Univ & Res, Phys Chem & Soft Matter, Stippeneng 4, 6708 WE Wageningen, Netherlands
[c] School of Food Science and Biotechnology, Zhejiang Gongshang University, Hangzhou, Zhejiang 310018, China

HIGHLIGHTS

- Henry's constant is obtained from the results of Self-Consistent field calculations to compare the surface affinity of amphiphilic copolymers of various architectures.
- Spatial distribution of adsorbing segments along polymer chains has great influence on their adsorption and ultimately on colloidal stabilising properties, when used as dispersants.
- For star-like polymers with identical chemical compositions, the surface affinity decreases with increasing number of arms.
- For amphiphilic copolymers of the same chemical composition, dendritic polymers have the highest surface affinity.

GRAPHICAL ABSTRACT

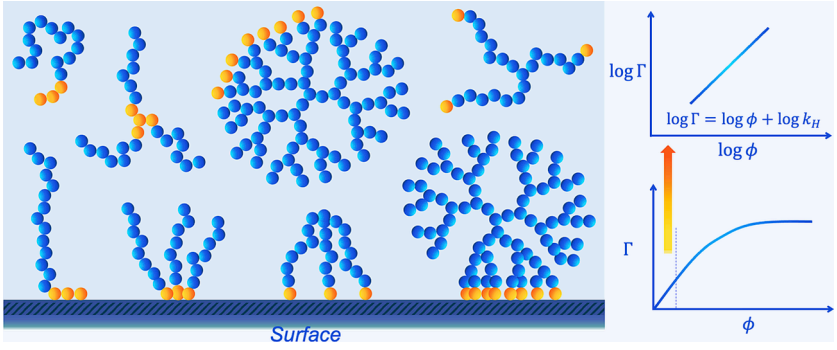

ARTICLE INFO

Keywords:
Amphiphilic copolymers
Polymer surface adsorption
Colloidal dispersions
Polymer architecture
Henry's constant
Self-Consistent field (SCF)

ABSTRACT

Hypothesis: Polymer architecture is known to have significant impact on its adsorption behaviour. Most studies have been concerned with the more concentrated, "close to surface saturation" regime of the isotherm, where complications such as lateral interactions and crowding also additionally affect the adsorption. We compare a variety of amphiphilic polymer architectures by determining their Henry's adsorption constant (k_H), which, as with other surface active molecules, is the proportionality constant between surface coverage and bulk polymer concentration in a sufficiently dilute regime. It is speculated that not only the number of arms or branches, but also the position of adsorbing hydrophobes influence the adsorption, and that by controlling the latter the two can counteract each other.

Methodology: The Self-consistent field calculation of Scheutjens and Fleer was implemented to calculate the adsorbed amount of polymer for many different polymer architectures including linear, star and dendritic. Using the adsorption isotherms at very low bulk concentrations, we determined the value of k_H for these.

Findings: It is found that the branched structures (star polymers and dendrimers) can be viewed as analogues of linear block polymers based on the location of their adsorbing units. Polymers containing consecutive trains of adsorbing hydrophobes in all cases showed higher level of adsorption compared to their counterparts, where the hydrophobes were more uniformly distributed on the chains. While increasing the number of branches (or arms

* Corresponding authors.
E-mail addresses: mingduo.mu@mail.mcgill.ca (M. Mu), r.ettelaie@leeds.ac.uk (R. Ettelaie).

https://doi.org/10.1016/j.jcis.2023.04.051
Received 27 October 2022; Received in revised form 5 April 2023; Accepted 12 April 2023
Available online 18 April 2023

for star polymers) also confirmed the known result that the adsorption decreased with the number of arms, this trend can be partially offset by the appropriate choice of the location of anchoring groups.

1. Introduction

Adsorption of polymers onto solid surfaces is of great importance due to its practical implication in colloid science, lubrication, surface treatment, controlling surface wettability, and in design of biocompatible films [1–4]. In relation to emulsions, the "surface" considered in both experimental and theoretical studies are often taken as a hydrophobic surface, mimicking an otherwise non-solid oil–water interface. A good emulsifier needs to be surface active so that it can rapidly adsorb onto the interface and reduce the surface tension. In real life applications, to ensure colloidal stability of the droplets, it is often important to saturate the surfaces with emulsifiers, i.e., to have a reasonably high surface loading, but without excess emulsifier remaining in the solution so as to be detrimental to system stability [5,6]. This requires the molecules to have amphiphilic structures, containing both hydrophobic and hydrophilic segments. The driving force for such adsorption is a combination of hydrophobic interactions and the low solubility of hydrophobic segments of the macromolecules in aqueous environment. Apart from synthetic co-polymers, in foods, agrochemicals, pharmaceuticals, and other biologically related types of applications, proteins and hydrophobically modified polysaccharides are also particularly good examples of amphiphilic bio-macromolecular emulsifiers [5]. In recent years, experimental studies on hydrophobically modified starch have found that the ratio of linear and branched starch molecules (amylose and amylopectin) has a significant impact on the emulsifying behaviour of the modified starch [7–9], which leads to a more general and fundamental question as to what influence does the chain architecture have on the adsorption behaviour of such amphiphilic copolymers?

Henry's constant (k_H) is often encountered in relation to the adsorption behaviour of low molecular weight surfactants. It refers to the constant of proportionality between the surface coverage and bulk concentration in a sufficiently dilute regime. However, all amphiphilic molecules, including the much larger polymeric ones, also obey Henry's law provided that the degree of the surface coverage remains low, i.e. in the limit where the adsorption of a molecule onto the surface is not influenced by the presence of other neighbouring molecules. Therefore, in such a case the lateral interactions between adjacent chains remain negligible. For amphiphilic polymers k_H tends to be very large. This, combined with much larger size of polymers, means that any overlap between neighbouring chains develops rather quickly, even at a relatively low level of surface coverage. This limits the validity of Henry's regime to very dilute solutions, making a precise experimental determination of Henry's constant for these molecules quite tricky. Nonetheless, as we demonstrate further below, there are many practical situations for which such low dilutions do occur, even where the total amount of polymer in the entire system is by no means negligible. The cases in mind involve systems with very high specific surfaces, such as fine colloidal dispersions or small emulsion droplets.

In some instances, the effect of chain architecture has been investigated in the context of modification of surfaces. Films close to their maximum monolayer coverage (i.e. brush like films) are formed when the surface is saturated with polymers. These have been studied in relation to the impact that the architecture of a grafted polymer can exert on the subsequent adsorption of another entity (e.g. a protein) onto the grafted surface [10–13]. A well-known example is the surface treatment to prevent the attachment of molluscs and other aqueous organisms to the surface of ships, platforms, and marine structures under water [14–16].

Many attempts have also been made at deciphering the relationship between polymer architecture and the adsorption of chains themselves, both experimentally and through theoretical calculations. Experimentally, Bulychev et al. [17] studied the adsorption of amphiphilic linear polymers onto different surfaces and found that the adsorption layer formed by diblock linear polymers was thicker than that formed by multi-block linear structures of similarly sized chains. Trégouët et al. [18] focused on the dynamic properties of interfacial layers formed by polymers, possessing various lengths and grafting densities for their adsorbing hydrophobic segments. It was found that at high grafting densities, the adsorbed layers incur a larger elastic penalty upon compression and therefore these polymers desorb faster as compared to those with lower grafting densities. As for more complex structures such as amphiphilic combs, Tian et al. [19] focused on the scaling analysis in good solvents, and proposed that by using a branching parameter it is possible to describe the overall effect of branching of the chains on the equilibrium properties of the adsorbed layers of such comb-like polymers. Experimental studies have also been done to compare the linear and bottle-brush homopolymers of comparable molecular weights. Linear polymers were thought to form more extended adsorbed layers than their bottle-brush counterparts [20]. The same conclusion was also drawn from a theoretical study conducted by Ettelaie et al. [21], comparing linear and branched amphiphilic polymers representing simple models of hydrophobically modified amylose and amylopectin starch.

Experimental methods are time and resource bounded, and some parameters (e.g. degree and position of substitution in modified starch) and conditions (e.g. a theta solvent for glucose residues in starch) are hard to control or achieve in practice. In comparison, theoretical methods give us the essential tool to investigate more idealised conditions, and to focus on a specific parameter of interest, without altering others. For example, the transition from weak to strong adsorption can simply be achieved by increasing the strength of monomer-surface interaction [22–25] without changing size or architecture of chains. Similarly, the degree of polymer overlap on the surface can be adjusted to a desirable level by varying its bulk concentration to low values, not always feasible to study in practical situations.

When polymers adsorb onto a surface, the adsorption amount is limited by the lateral interactions between the neighbouring molecules. For copolymer chains of interest here, this is usually the excluded volume interactions between the solvent loving parts of the chains. The full coverage scenario, involving saturated surface layers, has been studied both for homopolymers and in relation to amphiphilic macromolecules. Recently, Leermakers et al. [26] focused on the saturated adsorbed regime for homopolymers comparing various chain architectures with each other. In this study the de Gennes scaling exponent [27,28] for polymer density in the central region of the adsorption layer was characterised. It was also concluded that comb-like polymers are better at providing colloidal stabilization than their symmetrically branched counterparts, in that they mediate a stronger steric repulsion between colloidal particles which have been covered by them.

In many studies the interest was drawn to the conformations taken by polymers at an interface. The distribution or length of trains, loops, tails are often characterised, and structures with long tails are known to form thicker adsorbed layers [21–23,26,29]. Besides other factors such as solvent quality and adsorption strength, the location or distribution of the adsorbing units along the copolymer backbone also has a major influence on the polymer conformation adopted by the chains on the surface. As such then, the location of hydrophobic anchoring groups also strongly affects the thickness of the resulting adsorbed layers [30,31].

Here we would like to focus on another aspect characterising the adsorption properties of polymers, by mainly examining the very dilute regime (i.e. the mushroom adsorption regime [32,33]). That is to say we are interested in the low bulk-concentration/below-saturation surface

coverage part of the adsorption isotherm. However it is important to realise that a very low equilibrium dilute aqueous solution in the system does not necessarily imply a system that is abnormally low in polymer content. For example, consider a typical O/W emulsion formulation containing a volume fraction $\varphi_{oil} = 0.40$ of oil, dispersed as fine oil droplets in water (radius R = 0.25 μm) stabilised by a macromolecular emulsifier (e.g. protein in foods or pharmaceutical type applications). The specific interfacial area between oil and water (S) is

$$S = \varphi_{oil}\left(\frac{4}{3}\pi R^3\right)^{-1}(4\pi R^2) = \frac{3\varphi_{oil}}{R} \tag{1}$$

i.e.4.8 × $10^6\, m^{-1}$ or $4800\, m^2$/L for the above system. Most amphiphilic macromolecules, such as proteins, have a very high degree of surface affinity and will almost completely adsorb at oil–water interfaces, hence leaving little excess polymer present in the aqueous solution. Therefore, taking the protein solution used in making such formulations to be of 5.0 g/L protein (again quite representative in such applications), the polymer surface coverage is

$$\Gamma = \frac{C_p \times \varphi_{ps}}{S} \tag{2}$$

where C_p is the concentration of protein solution, and φ_{ps} the volume fraction of the protein solution = 1-φ_{oil}. For our typical system this evaluates to 0.63 mg/m^2, which is quite a bit below the 1 mg/m^2 saturation surface coverage often reported for proteins of various kinds in the literature [34]. Therefore, in such a practically encountered system, once the equilibrium between bulk solution and the surface of droplets is attained, the aqueous solution will have extremely low protein concentrations, not too dissimilar to the ones considered in this study. It is our aim to calculate Henry's constant k_H for different architectures and use this to compare the inherent adsorption property of given chain, purely arising from its structure as opposed to the crowding and interactions between neighbouring polymers. More specifically, we aim to investigate the impact of a particular polymer architecture on the affinity of the chain for adsorption on the surface. Linear, star, and dendritic structures are investigated and compared here. We hope that the results will prove useful in the design of more tailored amphiphilic macromolecular emulsifiers, at least in cases involving synthetic amphiphilic copolymer. Similarly, our study should prove useful in providing further insight into behaviour of different biomacromolecular architectures at interfaces, of which hydrophobically modified starch (involving both linear amylose and branched amylopectin) is a typical example.

2. Methodology

2.1. Self-Consistent field calculations

The Scheutjens and Fleer formulation of Self Consistent Field theory can be applied to complex copolymers [1,35] and has been used extensively to study the surface adsorption behaviour of such macromolecules [21,36–41]. This model considers two parallel flat surfaces with the gap between them filled with a solution of polymers. The space between the two surfaces is subdivided into a lattice (cubic one in our case here) and each cell is occupied by either a monomer (belonging to chains) or a solvent molecule. No atomic details regarding actual size or shape of monomers are taken into account in this coarse-grained view of the chains, much in the same way as the lattice Flory-Huggins model of polymers. However, the Flory-Huggins interaction parameters between the monomers, solvent and the surfaces are specified to reflect their affinity for each other and thus also broadly reflecting their chemical nature. The polymers are considered fully flexible with a Kuhn length that is small compared to the length of any branches. The adsorbed amount onto the interface can be calculated from the density profiles at any given bulk volume fraction, provided that the two surfaces are placed far apart so as not to affect polymer adsorption occurring on each other.

The details of the SCF theory, and Scheutjens and Fleer formulation of it, have appeared in many previous reviews and publications and will not be repeated here [36,42,43]. But briefly, the calculations start by averaging the molecular degrees of freedom (position of monomers) which yield a free energy functional, $F(\{\phi_i^\alpha(r)\})$, specifying the free energy for any arbitrary given set of density profiles $\{\phi_i^\alpha(r)\}$ between the two surfaces [44,45]. Here $\phi_i^\alpha(r)$ denotes the volume fraction of the monomer residue of kind α, belonging to chains of type *i*, at a distance *r* away in the gap. The distance *r* is measured perpendicularly relative to one of the surfaces, expressed in units of segment size. The free energy functional includes both the enthalpic contribution, arising from the interaction of chains with each other and with the solvent molecules, as well as the entropic term capturing all the possible configurations of the chains that lead to the same specified set of density profiles $\{\phi_i^\alpha(r)\}$.

During the derivation of the free energy functional, a set of auxiliary fields $\psi_\alpha(r)$ also enter the calculations. These fields need to be the ones that project out the same density profiles for which the free energy is being calculated (in an equivalent system in which all internal interactions are switched off). In principle the free energy of the system is then obtained in the usual way by calculating the partition function through summation over all plausible density profiles:

$$\frac{F}{k_BT} = -\ln(Z) \simeq -\ln\left[\int \exp\left(-F(\{\phi_i^\alpha(r)\})/k_BT\right) D\phi_i^\alpha(r)\right] \tag{3}$$

where *Z* is the partition function of the polymer solution and $\{D\phi_i^\alpha(r)\}$ indicates that we are taking a functional integral over all possible functions of $\phi_i^\alpha(r)$. Each density profile has an associated probability of occurrence proportional to $\sim \exp(-F(\{\phi_i^\alpha(r)\})/k_BT)$. The essential approximation in SCF theory is then that the summation in eq. (3) is assumed to be completely dominated by the most probable profile set, which obviously occurs when functional $F(\{\phi_i^\alpha(r)\})$ attains its absolute lowest value. Thus, the problem of determining the free energy of the system reduces to one of searching for a minimum for $F(\{\phi_i^\alpha(r)\})$.

With the above approximation, instead of averaging the thermodynamic quantities of interest over all of the possible sets of density profiles, here one takes these to be the values given by the density profile with the lowest free energy. Any fluctuations around the most dominant profile are thus ignored, as is the case with other mean field type theories. The calculations for obtaining the most probable density profile set is well described in many articles in the literature. In most of these, it is carried out through an iterative numerical procedure [1,26,44,46], which often also involves the imposition of the incompressibility condition where

$$\sum_i \sum_\alpha \phi_i^\alpha(r) = \sum_i \sum_\alpha \Phi_i^\alpha = 1 \tag{4}$$

for all *r* values. It is possible to show that the profiles and their corresponding auxiliary fields satisfy the following relation when the minimum free energy occurs

$$\psi_\alpha(r) = \psi_h(r) + \left(\sum_\beta \chi_{\alpha\beta} < \sum_i \phi_i^\beta(r) > \right) + \chi_{\alpha s}[(\delta(r) + \delta(r-L))] \tag{5}$$

where $\delta(r)$ represents the Dirac's delta function (becoming Kronecker-delta function in the discretised model used in the actual numerical computation), $\psi_h(r)$ is a hard core potential that ensures the incompressibility of the system as imposed by eq. (4), and $\chi_{\alpha\beta}$ is the Flory-Huggins interaction parameter between species α and β [44]. The interaction between a monomer of kind α and the surface is given by $\chi_{\alpha s}$. The values of the auxiliary fields at this stage can be said to correspond

to those felt by a monomer (or solvent molecules) due to their interactions with the neighbouring species. Once the calculations are completed, that is when the axillary field and density profile satisfy eq. (5) to a required degree of accuracy, any thermodynamic quantity of interest can be obtained from the resulting set of density profiles. Some further details on the implementation of the scheme can be found in the Supporting Information SI.2.

2.2. Modelled polymer architectures

The polymers considered here consist of two types of monomers only, the hydrophilic ones that prefer staying in the solvent, and the hydrophobic residues that favour adsorption onto the surface. The solvent molecule, hydrophilic monomer, hydrophobic monomer, and the surface are denoted as species type 0, 1, 2, and s respectively. Three types of polymer architectures are examined and compared here, linear, star-like, and dendritic polymers. They are schematically illustrated in Fig. 1A. For simplicity the hydrophobic monomers are not separately highlighted on these diagrams. The first structure is a basic linear chain (Fig. 1Aa), where the polymers are designed as being diblocks. The molecular weight for the linear and all the star polymers are kept the same, at 400 total monomers. For star-like polymers, while they all have the same molecular weight, the number of arms varies from 3 to 7 (Fig. 1Ab). This obviously means that the more arms that there are, the shorter each arm would be. The dendritic polymers (Fig. 1Ac) are designed to have a core section beginning with a 3-armed star, thus avoiding a long linear region at the central part. The individual strands are of equal length, each being 40 monomers. Apart from the central 3-arm core, bifurcation at all other branching points are kept at 2. Number of generations (i.e. the number of bifurcation starting from core, as one moves down towards the tips) considered are 2, 3, 4 and 5, thus giving the total number of monomers for the studied dendritic chains as 361, 841, 1801, 3721. The corresponding number of free ends for these are 6, 12, 24, 48, respectively. The monomers belonging to each generation as we move away from the root (i.e. core section) are coloured differently in Fig. 1Ac, to better demonstrate this considered structure.

The degree of hydrophobic modification is kept at the same level for all the star and dendritic architectures. This is set at one hydrophobic monomer out of every 40 residues. This results in each star-like polymer having 10 hydrophobes, regardless of the number of their arms. For dendritic chains, each linear strand contains on average one hydrophobe, thus leading to a total of 9, 21, 45 and 93 hydrophobes in dendrimers of increasing complexity, with generation numbers 2, 3, 4 and 5, respectively.

In order to investigate the role of the position and distribution of hydrophobic monomers along the chain backbone, these are varied within each polymer architecture type. Based on the spatial distribution of hydrophobic monomers on the backbone, these can either all be placed as a single block on one segment of the structure (i.e. all hydrophobes are connected to each other), or positioned as a larger number of blocks, each having a smaller numbers of hydrophobic monomers, distributed along several different segments (Fig. 1B, a, b versus c). Furthermore, hydrophobic monomers can be located either at the centre, or at the free ends of the structures (Fig. 1B, b versus a, c).

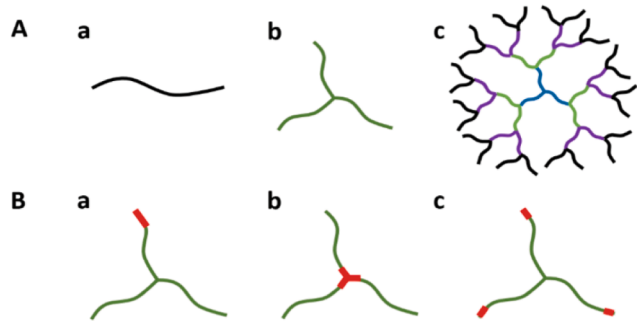

Fig. 1. A. Schematic illustrations of the three models used in this work, without highlighting the hydrophobic monomers explicitly; (a) linear structures with no branching points. (b) star polymers with arms of equal length (example shown has 3 arms), (c) symmetrical dendrimers of generation g, with a starting branching of 3 at the root, followed by a bifurcation of 2 at each branch point further down towards the tips. Each individual linear strand between any two branch points has 40 monomers. The example here shows a chain with 4 generations, and thus 45 linear segments. **B.** Schematic illustration of the position of hydrophobic monomers in studied star polymers. Position of hydrophobes are highlighted here with thick red lines. Here a 3-arm star is presented as an example. Hydrophobic monomers are (a) positioned at a free end on one arm only; (b) evenly distributed among all arms, placed at the centre; (c) evenly distributed among all arms, with all the hydrophobes located at the free ens. (For interpretation of the references to colour in this figure legend, the reader is referred to the web version of this article.)

2.3. Adsorption isotherm and Henry's constant

The surface affinity of the above structures is characterised by Henry's constant k_H, specifying the constant of proportionality between the adsorbed amount and the bulk concentration, in the limit of very low dilution. As such, k_H reflects the inherent adsorption properties of single individual chains, without the complication of their interactions with the neighbouring polymers, when adsorbed. The value of k_H is related to the free energy change, ΔG, upon adsorption of a single chain:

$$k_H \propto \exp\left(\frac{-\Delta G}{k_B T}\right) \tag{6}$$

where $\Delta G = \Delta H - T\Delta S$ includes both an enthalpic term ΔH and an entropic term ΔS. For a single monomer, the entropic change upon its adsorption onto the surface is normally assumed to be 0 (making the reasonable assumtion that the internal configuration of a small molecule on surface is not all that different to when it is in bulk). Therefore, for molecules comprising of a single monomer α, k_H is solely dependent on the enthalpic term

$$k_H = \exp(-\chi_{\alpha s}) \tag{7}$$

where $\chi_{\alpha s}$ is the Flory-Huggins interaction parameter between the monomer α and surface (relative to that between the monomer and the solvent, i.e. χ_{0s} is always 0). However, for polymeric chains the entropic term S can make a significant contribution. As the chains adsorb onto the surface, they lose configurational entropy due to restrictions presented by the proximity to the interface. Therefore, the relation in eq. (7) only remains true in cases where the entropic change stays constant for the adsorbing entities.

Here we choose to calculate k_H according to the adsorption isotherm instead of directly from ΔG. Prior to applying the method to more complicated structures such as stars and dendrimers, it is useful to first validate the approach using several simpler cases. For these a prediction for the value of k_H, or its variation with χ_{cs}, number of hydrophobes, or other similar parameters, can feasibly be made. Dimers and simple amphiphilic linear chains are chosen as model structures for this validation, with their k_H either analytically calculated or known to follow a predictable trend.

The adsorbed amount is given as follows

$$\Gamma^{exc} = \frac{1}{N}\int_0^\infty (\boldsymbol{\phi}(r) - \Phi_{bulk})\boldsymbol{dr} \tag{8}$$

where Γ^{exc} is the adsorbed number of chains, defined here as the integral of the excess amount of polymer up and above that in the bulk. In eq. (8), N is the number of monomers in a polymer, $\phi(r)$ is the volume fraction at r, and Φ_{bulk} is the volume fraction of the polymer in bulk solution.

From the SCF calculations discussed in the previous section, the

adsorbed amount for a range of bulk polymer concentrations (or volume fractions, as normally specified here) can be obtained. Using these the adsorption isotherm is determined by plotting the adsorbed amount vs. bulk volume fraction. A full isotherm is expected to broadly exhibit features resembling a Langmuir isotherm. At very low concentration, adsorption increases linearly with bulk concentration as chains adsorb independent of each other. As the bulk volume fraction increases, the surface starts to become saturated with polymers. Lateral interactions between adsorbed chains on the surface make further increments in adsorbed amount more difficult, leading eventually to a plateau at higher bulk polymer concentrations [47]. This is considered to result in a transition from the so-called "mushroom" to the "brush" regime, as surface loading increases for copolymers [32,33].

Here we mainly focus on the dilute or the "mushroom" regime of the adsorption isotherm, where the linear relationship between adsorbed amount and bulk concentration is valid. In this regime, polymers do not overlap with each other and behave as individual isolated molecules on the surface. As such, at this very low adsorption level, the excluded volume interactions between the adjacent adsorbed chains are usually not significant. Nevertheless, to further switch off the effects of any excluded volume interactions, we set the interaction parameter between the hydrophilic monomer and solvent molecule to $\chi_{10} = 0.5$. Therefore, in doing so we assume that the solvent is a theta solvent for the hydrophilic parts of the chains, so that the chains can be regarded as Gaussian chains in the solution, rendering our calculation valid on the level of a qualitative analysis. It is worth noting that the presence of three body interactions, still present at theta-point, has not been considered in this study and needs further examination [48,49]. However, since the polymers examined here are amphiphilic, one expects that factors such as the location of hydrophobic entities will exert far more influence on the adsorption behaviour of the polymers at theta point rather than these possible three body term corrections. Henry's constant k_H is obtained from the slope of the linear part of our calculated isotherm, $\Gamma = k_H\phi$, where Γ is the amount of surface coverage and ϕ the bulk polymer volume fraction, or alternatively from

$$\boldsymbol{log}_{10}\Gamma = \boldsymbol{log}_{10}\boldsymbol{\phi} + \boldsymbol{log}_{10}\boldsymbol{k_H} \tag{9}$$

When adsorbed amount is plotted against volume fraction on a logarithmic graph, a straight line is expected with the slope equal to 1 in the linear part of the isotherm. We use this as a test to make sure that the calculations were performed for sufficiently dilute solutions.

For simple monomers, the value of k_H is shown above to be $k_H = \exp(-\chi_{as})$. However, for complex polymeric chains, their entropic change upon adsorption complicates the relation and as a result k_H often cannot be calculated analytically. The above relationship for such polymers merits more complex SCF calculation, as a possible way for obtaining k_H for these more sophisticated structures than simple monomers. This work intends to determine and compare Henry's constant for a range of chemically identical, but otherwise structurally different copolymers to explore and understand the contrasting adsorption behaviour which arises solely from polymer chain architecture.

3. Results and discussion

In this section, we first verify the proposed method above by obtaining k_H for dimers and certain amphiphilic linear polymers, where surface affinity is more predictable. The validated method is then extended to examine and contrast more complex structures: amphiphilic linear, star and dendritic type polymers.

3.1. Verification of the method

3.1.1. Dimers

We first verify the method by applying it to some simple structures whose k_H can be calculated analytically. We stress that the examples in this section are merely used to allow for the verification of the method, rather than being realistic models of any specific molecules per se.

Two types of dimers are considered here as the simplest structures suitable for the verification of the method. The first case is a dimer of two adsorbing hydrophobic monomers, and the second is a dimer consisting of one adsorbing hydrophobic monomer and one non–adsorbing hydrophilic monomer. In both cases, each hydrophobic monomer has an interaction strength (χ_{2s}) with the surface, defined in units of k_BT, as is customary. This is varied from -2 to -5. In the second case, to ensure that we can engineer a model situation where dimers predominately adsorb "perpendicular-to-surface", the hydrophilic monomer is assigned a highly unfavourable interaction parameter of $\chi_{1s} = +9$ with the surface. Note that this is chosen in this section to allow an analytic independent determination of Henry's constant to be undertaken for the purpose of comparison with our numerically calculated data. However, such highly unfavourable unrealistic interactions values are not used in any of the following sections. Furthermore, the solvent is assumed to be an athermal one, with $\chi_{\alpha 0} = 0$ for both types of monomers. Thus, the hydrophobic monomer would adsorb to the surface, whereas the hydrophilic monomer strongly prefers to stay away from the surface.

In the Henry's regime, the interfacial layer formed by adsorbing dimers in the dilute solutions is only 2 layers thick at most. As remarked before, this makes it convenient to calculate the adsorbed amount, and hence k_H, analytically by considering the possible configurations that the dimer may adopt on the surface. Detailed calculation are shown in SI.1. In short, for the first case of two hydrophobic monomers, the "parallel to surface" adsorbed configuration dominates and Henry's constant can be calculated as.

$$\boldsymbol{k_H} \approx \frac{4}{6}\boldsymbol{\exp}(-2\boldsymbol{\chi}_{2s}) - 1 \tag{10}$$

In the second case, the "perpendicularly" adsorbed configuration dominates and the predicted value of Henry's constant is then

$$\boldsymbol{k_H} \approx \frac{1}{6}\boldsymbol{\exp}(-\boldsymbol{\chi}_{2s}) - 1 \tag{11}$$

The analytically calculated results can be compared to adsorption isotherms of these molecules, as obtained from our SCF calculations presented in Fig. 2. The constant c of the fitted lines (y = ax + c) to the plots of logarithm of surface coverage (y) vs. logarithm of bulk concentration (x) provide $\log_{10}(k_H)$ values. The lower limit of the accessible volume fraction is bounded by the computational accuracy of our program. The upper limit is constrained by physical considerations, i.e., when the adsorption isotherm begins to deviate away from the linear regime governed by Henry's law. The k_H values so obtained are listed in Table 1 for various values of χ_{2s}, together with the analytical values for comparison.

The two sets of predicted k_H values are in good agreement with each other. The analytically determined value of k_H is expected to be slightly lower, because of the approximation made here (see SI.1).

From the above results, we can see that the method proposed here for determining k_H, based on the use of SCF calculations, is able to provide sensible values, in line with expectations for these simple "test" dimers.

3.1.2. Results for linear amphiphilic polymers

The next set of structures employed for testing the methodology involve linear diblock polymers. With the length of hydrophilic segments now made much larger than the hydrophobic anchoring groups, the following calculations are performed for the theta solvent case ($\chi_{10} = 0.5$ for the hydrophilic monomers). It is worth noting that here the solvent strength for hydrophobic monomers is set as $\chi_{20} = 0$. Having a "hydrophilic" solvent favouring the solvent-hydrophobe interactions above solvent-hydrophile interactions, is usually not achievable in practice. However, as we had emphasised previously, in this section we wish to seek model systems that allow for validation of the method, rather than being a sensible representation of any specific system.

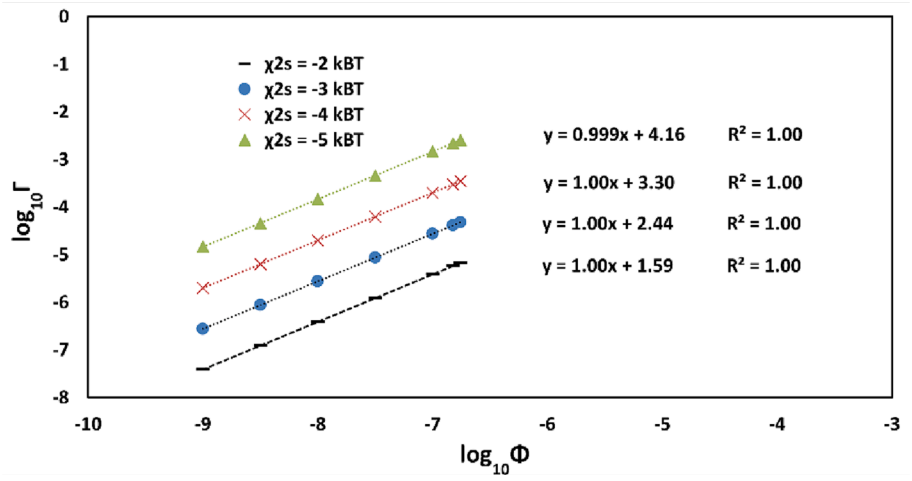

Fig. 2. Linear part of the adsorption isotherm for a dimer with a tendency to adsorb flat on the surface. The adsorbed amount is plotted against the bulk polymer volume fraction on a logarithmic scale. The equation and R^2 for the fitted linear regression line are included for each value of χ_{2s}, showing slopes that are very close to 1, as expected.

Table 1
The k_H determined from SCF and those obtained from analytical calculations, for dimers consisting of (a) two identical hydrophobic monomers, with χ_{2s} varied from −2 to −5, (b) one hydrophilic monomer ($\chi_{1s} = +9$), and one hydrophobic monomer (χ_{2s} varied from −2 to –5).

Composition of dimers	χ_{2s} of hydrophobe	k_H(SCF)	k_H(analytical calculations)
a. two hydrophobic monomers	−2	3.77×10^1	3.54×10^1
	−3	2.74×10^2	2.68×10^2
	−4	2.00×10^3	1.99×10^3
	−5	1.45×10^4	1.47×10^4
b. one hydrophobic + one hydrophilic monomer	−2	7.00×10^{-2}	2.30×10^{-1}
	−3	2.18×10^0	2.35×10^0
	−4	7.93×10^0	8.10×10^0
	−5	2.36×10^1	2.37×10^1

Setting $\chi_{20} = 0.0$ means that it is no longer necessary to consider the changes in the number of contacts between the anchoring groups and the solvent molecules, whether the former are in bulk or adsorbed on the surface.

The interaction potential of hydrophiles with the surface is kept at $\chi_{1s} = +9$ to ensure hydrophilic segments of the chains avoid lying on the interface upon adsorption of the chains. In this case, the linear diblock polymers should predominantly take the train-tail conformation on the surface (with very few loops present). For the same size of the hydrophilic blocks, and with their much smaller hydrophobic segments lying almost flat on the surface, the loss of configurational entropy of the hydrophilic part extending away from surface should be independent of the number of the anchoring hydrophobic residues. Of course this is only true when the degree of coverage is low (very dilute systems) and the adsorbed chains on the surface do not overlap, as is the case here. Above considerations make the relationship between the value of k_H and the adsorption energy more predictable. In the two systems studied below, the size of the hydrophilic block of the chains are kept constant. In the first case the hydrophobic block consists of just one monomer, but we vary the strength of the (favourable) interaction energy with the surface. In the second model, the χ interaction parameter for each hydrophobic monomer is kept the same, but the number of anchoring groups is altered instead.

The first linear diblock structure consists of 390 hydrophilic monomers, and as mentioned above has just one hydrophobe. The surface interaction parameter χ_{2s} for the hydrophobic residue is varied from −9 to –15. By keeping the number of the two types of monomers constant, and ensuring no contact between the hydrophilic segments and the surface (due to the high degree of unfavourable interaction between them, +9), one hopes to rule out any variation in the entropic contribution for different polymers, resulting from their adsorption. This then only leaves the enthalpic change to consider. Because there is only one hydrophobic monomer responsible for adsorption, the k_H is expected to then be proportional to the corresponding Boltzmann factor for adsorption of this monomer onto the surface, namely $k_H \propto \exp(-\chi_{2s})$ or

$$\ln(k_H) = -\chi_{2s} + a \tag{12}$$

where a is a constant.

Using graphs similar to those in Fig. 2, the value of k_H for chains with different χ_{2s} is determined from SCF calculation results. In Fig. 3a, the value of $\ln(k_H)$ is plotted against the Flory-Huggins parameter for the interaction of hydrophobic monomer with the surface. A clear linear relationship, with the slope very close to −1 and in good accordance with the prediction in eq. (12), is indeed obtained.

Another set of linear diblock amphiphilic polymers used here for the verification purpose, has a constant number of monomers in its hydrophilic block, in much the same way as that above (a total of 390). However, the number of hydrophobic monomers is now varied from 4 to 9, while the value of χ_{2s} is kept constant at −3. Again, by keeping the size and the nature of the hydrophilic part of the chains the same, and given that the hydrophobic part lying flat on the surface is only a small part of the chain, the entropic loss contribution to adsorption free energy for these structures are ensured to be almost identical. With higher number of hydrophobes, the loss of entropy as the chains adsorb becomes more significant. However, the enthalpic part is still predominantly accountable for the differences in k_H and thus the adsorbed amount for different chains. The variation in k_H here is the result of incremental addition of hydrophobes as we increase these from 4 to 9, in steps of one monomer at a time. With each addition the enthalpic component of the adsorption free energy changes by $\chi_{2s} = -3$ per chain. Therefore, for such a model $k_H \propto \exp(-\chi_{2s} \bullet n_{HB})$, where n_{HB} is the number of monomers in the hydrophobic block. In other words

$$\ln(k_H) = -\chi_{2s} \bullet n_{HB} + b \tag{13}$$

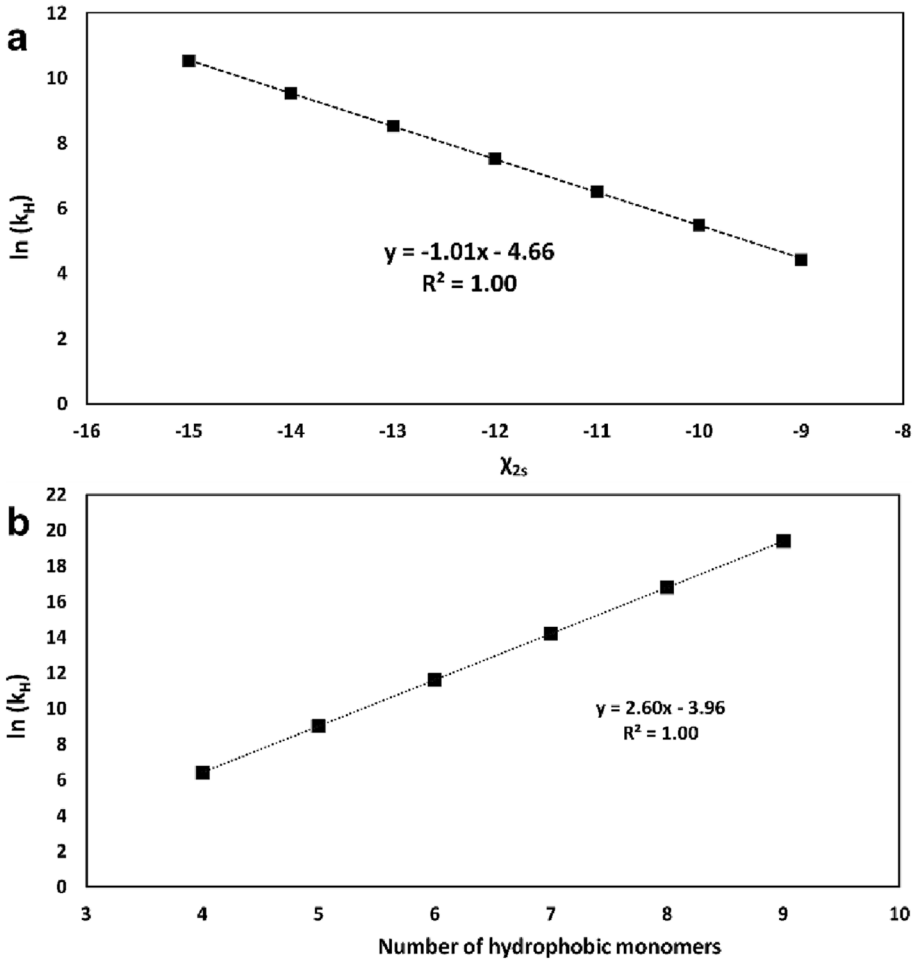

Fig. 3. (a) ln(k_H) plotted against χ_{2s} for linear amphiphilic polymers containing only one hydrophobic monomer, with χ_{2s} varied from –9 to −15. (b) ln(k_H) plotted as a function of the number of hydrophobic monomers, for a linear amphiphilic polymer. The number of monomers in the hydrophobic block varies from 4 to 9, but with χ_{2s} now kept constant at −3. The fitted straight line equations and R^2 values for the linear regression fits are also included.

where χ_{2s} is −3 and b is a constant. However, it must be noted that the entropy loss from the adsorbing hydrophobic block lying completely flat on the surface is also significant. At this point deviations from the expected slope of 3 are observed. For every additional hydrophobic monomer, 2 out of 6 orientations in our model are lost upon adsorption to the surface, giving a total change of $(\Delta H - T\Delta S)/k_BT = 3 - \ln(4/6) = 2.59$. Using our SCF calculations, we determined the adsorbed number of chains per surface as a function of bulk volume fraction. By considering the dilute regime, where the relation between these two quantities is linear, we obtained the values of k_H for systems with n_{HB} varying between 4 and 9. The procedure was identical to that used to obtain the results in Fig. 2. As shown in Fig. 3b, a plot of ln(k_H) versus the number of hydrophobic monomers (n_{HB}), produces the expected straight line with a slope of 2.60. This is in excellent agreement with the predicted value of 2.59 as was indicated above. Such an accordance suggests that the hydrophobic block is indeed lying quite flat on the surface, confirming that in this model the small adsorbing block adopts a train conformation with little or no loops. The results above also imply that by having the same length of hydrophilic block, the entropic loss of this part of the chain upon adsorption stays the same, irrespective of how strong the hydrophobic monomers are adsorbed onto the surface.

For both dimers and linear diblock amphiphilic polymers, the results of SCF calculations agrees closely with the predictions for these test models. With the approach for determining k_H having been shown to work well, we now apply the method to more complex chain architectures in the next section. For these, analytical prediction of k_H is not as straightforward as the model test cases above.

3.2. Adsorption constant for linear amphiphilic polymers

As the model is applied to more complex architectures, the Flory-Huggins interaction potential parameters are now chosen to be more representative of those we encounter in real systems wherever possible. From this point onwards, unless stated otherwise, the strength of interaction between solvent and hydrophilic residues is taken to be $\chi_{10} = 0.5$ while that with hydrophobic monomers is set at $\chi_{20} = 1$. Likewise, the χ interaction parameter between surface and the hydrophilic monomers is chosen to be $\chi_{1s} = 0$, which is more representative of hydrophilic residues in real systems.

The first structure examined is a linear amphiphilic chain containing identical number of hydrophobic monomers ($n_{HB} = 10$, with each having $\chi_{2s} = -2$). The magnitude of χ_{2s} is sufficiently large to ensure that the block of 10 anchoring monomers will lie flat on the surface. Hence, the adsorption energy associated with each linear chain on the surface is the same, irrespective of the length of its hydrophilic section. We alter this latter for the polymers from 10 to 390 monomers. Due to their unfavourable interaction parameter with the surface, the hydrophilic parts would avoid the interface and instead extend away from the surface into bulk solution, as shown in SI.3. Thus, at low levels of surface coverage (i.e. a very dilute solution) and with the enthalpic contribution remaining the same for chains of same hydrophobic block size, the main difference in free energy change upon adsorption is due to the entropic

term. The reduction in conformational entropy arises due to the restrictions that the impenetrable interface imposes on the adsorbed chains. For the set of different chains considered here then, this entropy loss should be a function of the length of the hydrophilic sections only [50].

A power law relationship is found between k_H and the hydrophilic block size of these polymers, with a R^2 value of 0.994 for the straight line fitted to ln(k_H) plotted against logarithm of the hydrophilic block size (Fig. 4). The relation is determined to be $k_H \sim (n_{HL})^{-\alpha}$ with the value of α close to 5/4. While having the same adsorption enthalpy, the linear chains with larger sizes tend to experience a greater level of conformational entropic loss upon adsorption. As a result, the value of Henry's adsorption constant k_H also decreases with increasing chain size.

3.3. Factors affecting the adsorption behaviour of branched polymers

3.3.1. Star-like polymers

In star-like polymers, both the number of arms and the position of hydrophobic monomers on these arms are possible factors affecting the adsorption behaviour of the chains. As before, we continue to take the strength of the interaction between the solvent and our hydrophilic and hydrophobic monomers as 0.5 and 1, respectively. All the star polymers considered here have the same number of monomers: i.e. 391 hydrophilic residues (with no affinity for the surface, $\chi_{1s} = 0$) and 10 hydrophobic ones (with preference for adsorption, $\chi_{2s} = -2$). The number of arms ranged from 3 to 7 in our study. Obviously, the larger the number of arms, then the shorter each arm will be. Having the same number of hydrophobic monomers, and provided that all these hydrophobic residues for an adsorbed chain do lie on the surface, the overall adsorption enthalpy should be independent of the number of arms. Furthermore, since we have chosen the chemical composition and the degree of polymerisation (at 400 monomers) to also be identical, then any differences in the adsorption constants must largely be attributed to differing levels of conformational entropy loss, when these star polymers with different number of arms are compared.

Three different positions of the hydrophobic monomers are taken into consideration, as is schematically illustrated in Fig. 1B. The hydrophobic residues are either all placed together as a single block on one arm or are evenly distributed amongst all the arms. A further chain architectural variation studied here involves placing all the hydrophobes at the centre of the chain, while in another they are located at the free ends at the tip of each arm. It is worth noting that structures with hydrophobes on one arm are the only ones breaking the symmetrical design of the polymers. We emphasise that such a none-symmetrical structure is of course not available for studies involving equal-sized-armed homopolymers, and therefore a useful variation to include here.

Star polymers with their hydrophobic monomers in the central parts, but equally distributed among the arms (as indicated by thick red lines in chain architecture schematics, shown in Fig. 5), behave in an identical manner to chains with their hydrophobes placed only on one arm (data not shown) but still in the central part. On the other hand, for polymers with hydrophobic monomers at the free ends (solid and dash-dotted curves in Fig. 5), the distribution of hydrophobes between different arms is found to greatly influences the affinity of the copolymers for adsorption onto the surface. Polymers with hydrophobic monomers equally distributed among all free ends had a value of k_H two orders of magnitude lower than those with all hydrophobes concentrated at the free end of one arm only. This observation resembles the well-known phenomenon for linear diblock polymers, where the diblocks adsorb more strongly than their triblock counterparts, while both possessing the same size and chemical composition [46]. Structure (a) in Fig. 5, where the adsorbing monomers are concentrated at one free end somewhat resembles a diblock structure, in that it has a single large hydrophobic block. As such, its non-adsorbing segments are able to extend further away from the surface, thus to some extent escape the restrictions imposed by the presence of the impenetrable interface. Large sections of such chains behave as if they were in the bulk, with relatively smaller loss in conformational entropy upon adsorption. Structure (b) in Fig. 5 is more reminiscent of a triblock linear polymer having a single adsorbing segment in the middle, and its two non-adsorbing blocks shorter than the diblock counterpart. With these latter blocks unable to extend as far as those in structure (a), a higher conformational entropic penalty loss is expected upon adsorption. Structure (c) of Fig. 5 has non-adsorbing blocks of the same length as those in structure (b). However, because now these are connected at the single cross-link point at the centre of the star-shaped polymer (with the free ends of all arms being hydrophobic), the possible configurations of the individual arms are significantly restricted. For strongly adsorbing hydrophobes, each arm has its hydrophobic free end adsorbed on the surface, with the other end of the arm having to return to the same cross–link point (at some distance away from the surface) as that for all the other arms. It is clear that in this case the decrease in the number of accessible configurations upon adsorption is far more than if the anchoring groups where close to the centre (i.e. to the cross-link point) of the polymer. Consequently, the entropic penalty paid by structure (c), when adsorbed, is the highest among the three-star structures studied here.

A more extended plot of the calculated adsorption isotherm, showing the adsorbed amount at higher bulk concentrations for some of the polymers in Fig. 5, is displayed in SI.4, thus putting into prospective the dilute Henry's region of interest here. We use a similar technique to that

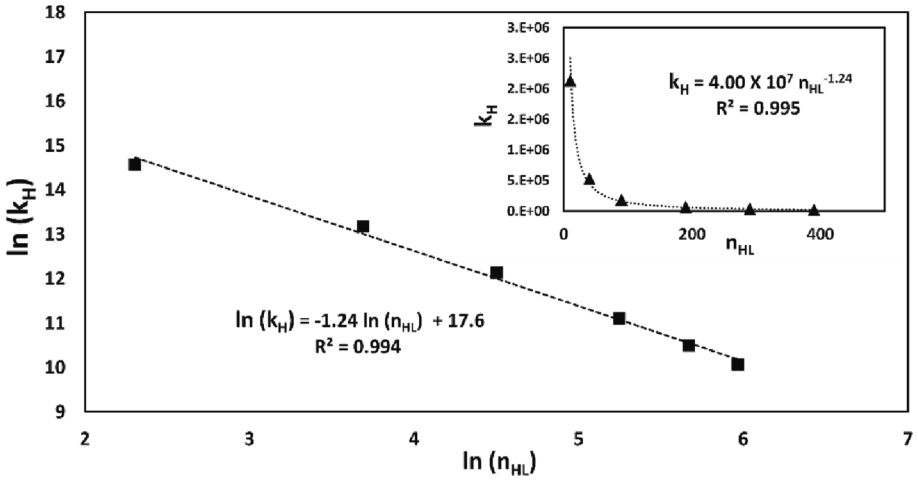

Fig. 4. Graph showing a power law relationship between k_H and the degree of polymerisation of the hydrophilic block (n_{HL}). Results are for linear diblock polymers each containing 10 hydrophobes, but with varying numbers of hydrophilic monomers ranging from $n_{HL} = 10$ to 390.

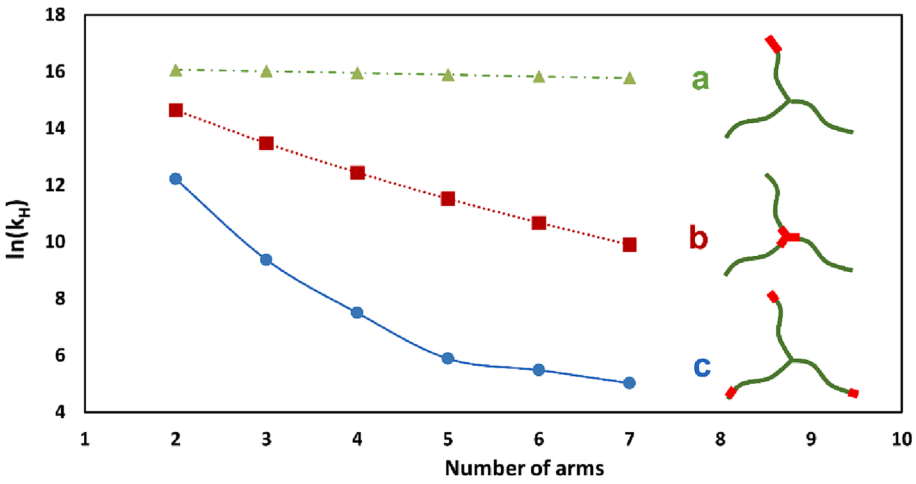

Fig. 5. The ln(k_H) of star polymers plotted against the number of arms, on a semi-log scale. Positions of hydrophobic monomers are: (a) concentrated on one arm only, at one free end, (b) evenly distributed among all arms, at the centre, and (c) evenly distributed among the arms, at all the free ends.

in Fig. 2 to obtain k_H for these star-like polymers. Generally all three star–like architectures in Fig. 5 show a decrease in the magnitude of k_H as the number of arms increases. This result is in agreement with previous reported data involving case (a) in Fig. 5, but obtained in more concentrated solutions in the brush regime [51]. However, more significantly, it is also found here that when the hydrophobic residues are placed as a single block on one end of a single arm, the decrease is seen to be only marginal (Fig. 5a) compared to other locations. This can also be seen from the average position of monomers belonging to the arm containing the hydrophobic groups, close to the surface (compare SI.5a to SI.5b and specially SI.5c). These are hardly altered as the numbers of arms is increased. There, the value of k_H remains large

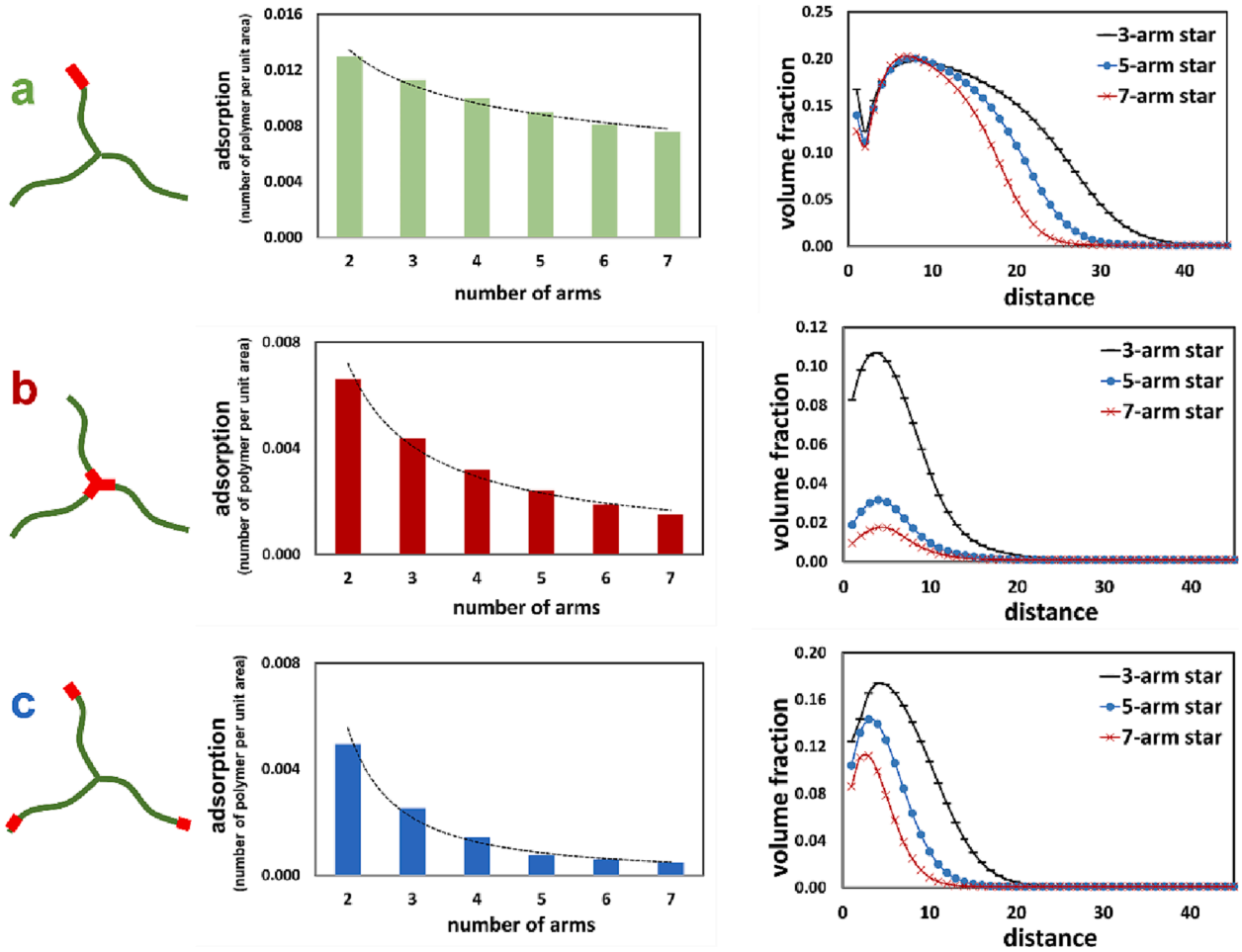

Fig. 6. Saturation surface coverage for three different star co-polymer architectures as displayed, as well as the corresponding volume fraction profiles (for the 3, 5 and 7 arm cases only), plotted against the distance away from the interface. All results are obtained at a bulk volume fraction of 10^{-3}, which now go beyond the Henry's regime of the isotherm.

compared to the other two star-shaped architectures studied, irrespective of the number of arms involved. As the number of arms increases, the hydrophilic blocks become smaller. However, the fact that any changes in k_H are small for structure (a), indicates that the arms remain reasonably long. In particular, it seems that the crosslink point can reside sufficiently far away from the surface. Thus, the presence of interface is only really felt by the single arm containing the anchoring groups. As far as all the other arms of the star-polymer are concerned, these remain sufficiently far from surface so as not to be much affected by its presence, or in turn influence the adsorption of hydrophobes belonging to the single anchoring arm (see SI.5a). This then provides an explanation for the modest decrease of k_H with the number of arms, as observed for polymer structure labelled (a) in Fig. 5.

Fig. 6 shows the maximum adsorbed saturation coverage for each star structure studied in Fig. 5. This is now at sufficiently high polymer bulk concentrations to ensure such surface saturation. The maximum coverage values are taken from the plateau regime of the adsorption isotherm. At this stage the variation of the adsorbed amount with any increase in bulk concentration is very small. Nonetheless, to have a more representative value, the adsorptions at bulk volume fractions of 10^{-4}, 10^{-3}, and 10^{-2} (all in the plateau regime) are averaged to obtain the surface coverage values presented here. In the same figure we have also displayed the SCF calculated results for the volume fraction profile for each polymer architecture possessing 3, 5 and 7 arms. In each case the polymer bulk volume fraction is set to be 1.00×10^{-3}. This bulk concentration was found to be sufficient for polymers to attain their saturation surface coverage, becoming limited by the overlap of neighbouring chains. As the number of arms increases, the adsorbed layers are seen to become more compact in all three cases. This is expected, since polymers with larger number of arms but the same molecular weight, are more compact entities than those with only a few arms. In turn, any overlaps between neighbouring adsorbed polymers within a more compact, less extended, interfacial layer increase more rapidly for chains with high number of arms. This tends to limit the number of adsorbed chains more strongly and keeps the amount of maximum coverage low. A clear decrease in the amount of adsorbed polymer, with increasing number of arms, is evident for all three cases presented in Fig. 6. In particular, it is interesting to note that this consideration applies as much to structure (a), where the anchoring groups are located only at the free end of one of the arms. The variation of the maximum adsorbed coverage with the number of arms is in stark contrast to the behaviour we observed in the low coverage end of the Langmuir-like isotherm for this latter polymer architecture. Recall (see Fig. 5a) that the value of k_H, characterising the adsorption at low bulk concentrations, was not overly sensitive to variation in the number of arms for chain structure (a), when the maximum surface coverage clearly seems to be so (Fig. 6a).

The other two star-shaped structures also have maximum surface coverages decreasing with an increase in the number of arms. The percentage decreases when arm number increases from 3 to 7 for three structures are (a) 41.7%, (b) 90.3%, and (c) 77.3%. The volume fraction for 7-arm stars, as one moves further away from the surface, also drops more quickly as compared to that of a 3-arm structure. For example, in case (a) the volume fraction for our 7-arm star returns to its bulk value at a distance of 32 monomer units away from surface. This is to be contrasted with a distance of around 48 monomer units for the 3-arm star polymers. The more rapid drop in the volume fraction of adsorbed chains, with increasing number of arms, is observed for all the three star-like structures that were considered here.

3.3.2. *Dendritic polymers*

As with the star polymers above, in this section the solvent strength for hydrophilic and hydrophobic monomers are once again maintained at 0.5 (i.e. theta solvent condition) and 1, respectively. Similarly, the strength of interaction with the surface for the hydrophobic monomers is kept at a favourable value of $\chi_{2s} = -2$, and that for the hydrophilic monomers is kept at $\chi_{1s} = 0$.

The dendritic polymers studied here have their overall monomer numbers increasing with generations. We define each generation to be the next level of branching in the tree-like structure for these polymers. Since the ratio of hydrophobic monomers to total monomers is kept at 1 to 40, polymers with a higher generation number now contain a larger number of hydrophobic entities, and as a result may be expected to also have higher k_H values. It is worth noting that the polymers in this study are designed to be flexible. Therefore, hydrophobic monomers, no matter where they are along the backbone, can be exposed and adsorb onto the surface. This consideration applies equally to hydrophobes at the very centre of the polymer.

Here five types of hydrophobic monomer distributions are considered, as illustrated in Fig. 7. The last two cases (d and e) are ones where the hydrophobes are equally distributed among all strands (one hydrophobic residue on each strand), being located either at the middle of each linear strand or next to the branching points. Both patterns would result in a lack of large single adsorbing blocks in these polymer architectures. As a matter of fact, the pattern where hydrophobic monomers are positioned in the middle of every strand (Fig. 7e) leads to a non-adsorbing behaviour of the polymer (data not shown), indicating that the adsorption potential is so weakened that essentially the chain loses its amphiphilic property altogether. On the other hand, in the case where hydrophobes are positioned next to each branching point (Fig. 7d), the amphiphilic nature is retained, allowing k_H to be successfully determined (Fig. 8d). The surface affinity of polymers with this pattern of spatial hydrophobic distribution does not alter much with the number of generations, or the size of the polymer. This is probably the result of the constant number of hydrophobic/hydrophilic monomer ratio (1 in 40 here) irrespective of the number of generations. The non-adsorbing segments in structure (d) of Fig. 8 cannot stretch very far away from the surface, with the polymer thus being forced to lie almost flat on the surface. As a result, chains with the structure (d) (Fig. 8) experience a very large degree of conformational entropic loss upon adsorption. Consequently, this structure is also found to have the lowest k_H values among the four shown in Fig. 8.

Dendrimers with the other three distribution patterns have their affinity for surface increased with the number of generations. For cases where hydrophobic monomers are at the free ends, the k_H value is higher for structure (b) where all hydrophobes are concentrated at 1/3 of the free ends in comparison to structure (c), i.e. the case with equal distribution of hydrophobes on all free ends. Here, dendrimer (c) can be likened to a triblock linear polymer whose central non-adsorbing segments extend away from the interface, but with the two anchoring free ends having to reside on the surface. Dendrimer (b) on the other hand, according to same analogy, resembles a similar behaviour to a diblock linear polymer, where those free ends without adsorbing monomers are free to extend away from the surface into the bulk solution. This is true for such structures of all generation levels. Much in the same way that a linear diblock chain has a higher k_H value than its triblock counterpart, here also we find the same for structure (b) relative to (c) (see Fig. 8).

The polymer with the highest surface affinity (i.e. largest k_H) here is found to be the one where all the hydrophobic residues are located at the central part, as a single continuous block (dendrimer (a) in Fig. 8). Though a linear analogue for dendrimer (a) is closer to a triblock polymer, this time the analogous triblock chain will have its anchoring groups in the centre, leaving the two non-adsorbing blocks on either side. It is found that k_H value for structure (a) is significantly higher than that for the dendrimer (b), especially with chains involving an increasingly larger number of generations. This is because structure (a) has all its outer branches freely extending away from the surface. The nature of dendrimer structure for the model used here, dictates that the number of linear strands (i.e. sections between two successive branching points) in each generation is twice that of the previous one. Our results here show that even if structure (b) had more extending free ends, the entropic loss associated with its adsorption is still larger than that incurred by

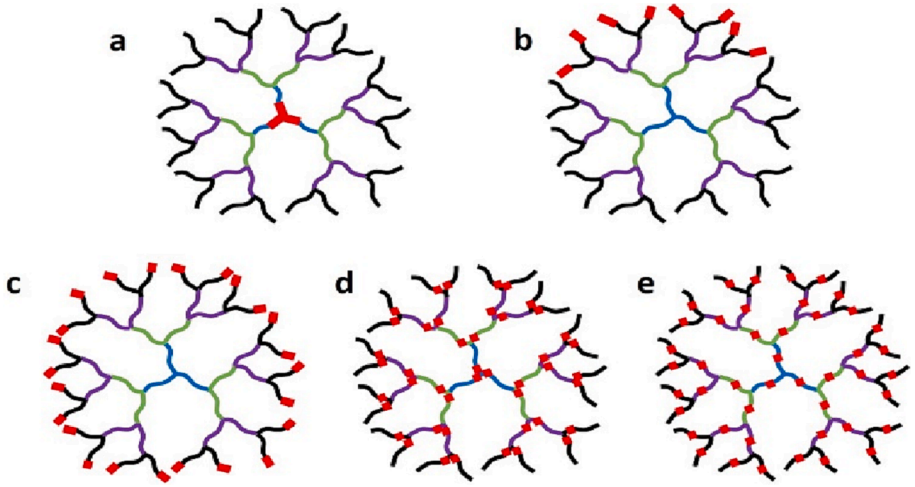

Fig. 7. Schematic illustration of the position of hydrophobic monomers in our model dendritic polymers, where these are highlighted with thick red blocks. For convenience the strands in each generation are coloured differently. Here a dendrimer with 4 generations (i.e. four levels of branching) is being displayed as an example. Hydrophobic monomers are (a) concentrated at the very centre of the polymer, with equal numbers on each of the three centrally connected strands; (b) distributed only among 1/3 of all the free ends; (c) evenly distributed at all free ends; (d) evenly distributed near each branching point; and (e) evenly distributed in the middle of each linear strand. (For interpretation of the references to colour in this figure legend, the reader is referred to the web version of this article.)

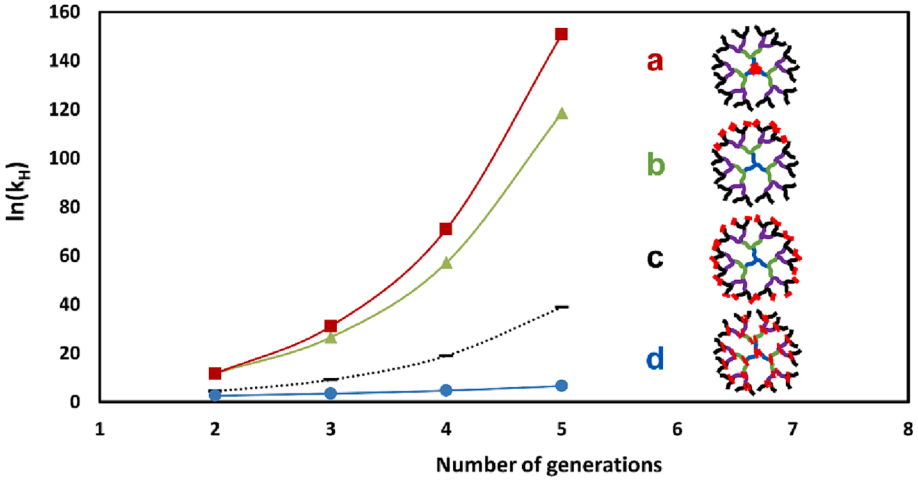

Fig. 8. The ln(k_H) for dendritic polymers plotted against the number of generations, on a semi-log scale. Positions of hydrophobic monomers are:, (a) concentrated at the centre, with equal number on each of the three strands joined in the middle; (b) distributed only amongst 1/3 of the free ends; (c) evenly distributed among all free ends; (d) evenly distributed near each branching point. The curves are guide to eye.

structure (a), where more segments are free to extend out. This is true even with shorter individual strands. Such distinctions in the adsorption behaviour of diblock and triblock structures are well known for linear polymers [46,52]. Here we have shown that the same can largely explain the behaviour of different dendrimer architectures, too.

It is clear that for both star-like and dendritic polymers, the spatial distribution and position of hydrophobic monomers on the polymer backbone greatly impacts their inherent surface affinity. In general, some of the principles applicable to linear chains seem to still hold for these much more complex structures. A less spread out and none-uniform distribution of hydrophobes, bunched into a fewer but larger blocks, results in a higher degree of adsorption affinity. Polymers resembling diblock linear chains (with one large single anchoring block) adsorb more than those resembling triblocks, multi–blocks or random co-polymers, if the chemical composition and numbers of hydrophobic and hydrophilic residues remain the same.

4. Conclusions

This study focused on the adsorption of polymers of various architectures in the initial linear end of the adsorption isotherm, and establishes a method for calculating Henry's constant k_H for amphiphilic polymers, using numerical SCF calculations. The method was first successfully validated by comparing the calculated k_H value obtained from SCF results and that obtained from direct analytical calculations, for several simple cases involving dimers or certain simpler linear polymer architectures. The approach is then applied to complex structures where k_H cannot be easily estimated from analytically calculations. To extend the range of structures previously examined in the literature [23,26], which have largely been homopolymers of various chain architectures, this study is conducted with amphiphilic copolymers. The entropic change for linear chains with constant number of adsorbing hydrophobic monomers, but with varying hydrophilic tails, is found to follow a power law with the size of the non-absorbing hydrophilic tails. The significance of the value of the power index remains to be determined. For star and dendritic polymers, different spatial distribution patterns of hydrophobic monomers along the chains is found to exert great influence on the surface affinity of the polymer. The position of anchoring groups directly impact the conformation of polymers on surface and the range that their non-adsorbing hydrophilic segments can extend away from the interface. The degree of branching and overall size of the polymers can exert a similar influence on the value of Henry's adsorption constant, again affecting the entropic restrictions incurred by the conformation of chains on the surface and their freedom to extend into the bulk solution. Such findings are in accordance with previous literature [21,23], involving either homopolymers of a range of

architectures or linear and dendritic copolymers resembling structures of hydrophobically modified starch. Other than the obvious application in providing information on the optimum position of hydrophobic residues added onto a hydrophilic backbone, the method can also be extended to look at pre-treated surfaces, as well as adsorption onto surfaces already covered by low molecular weight surfactants. By monitoring the change in Henry's constant of a particular macromolecule, insight can be obtained on the inherent adsorption affinity of this as the surface treatment is altered. Similar studies for disordered-coil like proteins, often used as emulsifiers in foods, can also prove of interest (see SI.6 for one such example). Such studies can bear significance for example in the design of industrial paints and coatings for marine structures, so as to prevent the attachment of sea molluscs and other such organisms.

CRediT authorship contribution statement

MM: Investigation, Methodology, Data curation, Formal analysis, Writing – Original draft, Writing – review & editing. **FAML:** Methodology, Validation, Writing – review & editing. **JC:** Conceptualization, Resources, Writing – review and editing. **MH:** Supervision, Resources. **RE:** Conceptualization, Methodology, Investigation, Formal analysis, Supervision, Writing – review & editing.

Declaration of Competing Interest

The authors declare that they have no known competing financial interests or personal relationships that could have appeared to influence the work reported in this paper.

Data availability

Data will be made available on request.

Acknowledgments

One of us (RE) wishes to thank B.S. Murray and M.Y. Janny for a number of useful discussions.

Appendix A. Supplementary material

Supplementary data to this article can be found online at https://doi.org/10.1016/j.jcis.2023.04.051.

References

[1] G.J. Fleer, M.C. Stuart, J. Scheutjens, T. Cosgrove, B. Vincent, Polymers at interfaces, Chapman & Hall, 1993.
[2] J.A. Hubbell, Bioactive biomaterials, Curr. Opin. Biotechnol. 10 (2) (1999) 123–129.
[3] M.G. Semenova, E. Dickinson, Biopolymers in food colloids: Thermodynamics and molecular interactions, CRC Press, 2010.
[4] S.R. Euston, Computer simulation of proteins: adsorption, gelation and self-association, Curr. Opin. Colloid Interface Sci. 9 (5) (2004) 321–327.
[5] E. Dickinson, Hydrocolloids as emulsifiers and emulsion stabilizers, Food Hydrocoll. 23 (6) (2009) 1473–1482.
[6] E. Dickinson, Hydrocolloids acting as emulsifying agents – How do they do it? Food Hydrocoll. 78 (2018) 2–14.
[7] X. Song, Y. Pei, W. Zhu, D. Fu, H. Ren, Particle-stabilizers modified from indica rice starches differing in amylose content, Food Chem 153 (2014) 74–80.
[8] M.C. Sweedman, J. Hasjim, C. Schafer, R.G. Gilbert, Structures of octenylsuccinylated starches: effects on emulsions containing beta-carotene, Carbohydr Polym 112 (2014) 85–93.
[9] M. Mu, P. Karthik, J. Chen, M. Holmes, R. Ettelaie, Effect of amylose and amylopectin content on the colloidal behaviour of emulsions stabilised by OSA-Modified starch, Food Hydrocoll. 111 (2021), 106363.
[10] D. Gingell, N. Owens, Inhibition of platelet spreading from plasma onto glass by an adsorbed layer of a novel fluorescent-labeled poly (ethylene oxide)/poly (butylene oxide) block copolymer: Characteristics of the exclusion zone probed by means of polystyrene beads and macromolecules, J. Biomed. Mater. Res. 28 (4) (1994) 491–503.
[11] C. Schroen, M.C. Stuart, K. Van der Voort Maarschalk, A. Van der Padt, K. Van't Riet, Influence of preadsorbed block copolymers on protein adsorption: surface properties, layer thickness, and surface coverage, Langmuir 11 (8) (1995) 3068–3074.
[12] C. Freij-Larsson, T. Nylander, P. Jannasch, B. Wesslén, Adsorption behaviour of amphiphilic polymers at hydrophobic surfaces: effects on protein adsorption, Biomaterials 17 (22) (1996) 2199–2207.
[13] K. Ishihara, K. Suzuki, Y. Inoue, K. Fukazawa, Effects of molecular architecture of photoreactive phospholipid polymer on adsorption and reaction on substrate surface under aqueous condition, J. Biomater. Sci. Polym. Ed. (2020) 1–19.
[14] L. Chen, Y. Duan, M. Cui, R. Huang, R. Su, W. Qi, Z. He, Biomimetic surface coatings for marine antifouling: Natural antifoulants, synthetic polymers and surface microtopography, Sci. Total Environ. 766 (2021), 144469.
[15] G. Dai, Q. Xie, X. Ai, C. Ma, G. Zhang, Self-Generating and Self-Renewing Zwitterionic Polymer Surfaces for Marine Anti-Biofouling, ACS Appl. Mater. Interfaces 11 (44) (2019) 41750–41757.
[16] J.H. Kardela, I.S. Millichamp, J. Ferguson, A.L. Parry, K.J. Reynolds, N. Aldred, A. S. Clare, Nonfreezable Water and Polymer Swelling Control the Marine Antifouling Performance of Polymers with Limited Hydrophilic Content, ACS Appl. Mater. Interfaces 11 (33) (2019) 29477–29489.
[17] N. Bulychev, B. Dervaux, K. Dirnberger, V. Zubov, F.E.D. Prez, C.D. Eisenbach, Structure of adsorption layers of amphiphilic copolymers on inorganic or organic particle surfaces, Macromol. Chem. Phys. 211 (9) (2010) 971–976.
[18] C. Trégouët, T. Salez, N. Pantoustier, P. Perrin, M. Reyssat, C. Monteux, Probing the adsorption/desorption of amphiphilic polymers at the air–water interface during large interfacial deformations, Soft Matter 15 (30) (2019) 6200–6206.
[19] P. Tian, D. Uhrig, J.W. Mays, H. Watanabe, S.M. Kilbey, Role of Branching on the Structure of Polymer Brushes Formed from Comb Copolymers, Macromolecules 38 (6) (2005) 2524–2529.
[20] A. Naderi, J. Iruthayaraj, T. Pettersson, R. Makuska, P.M. Claesson, Effect of polymer architecture on the adsorption properties of a nonionic polymer, Langmuir 24 (13) (2008) 6676–6682.
[21] R. Ettelaie, M. Holmes, J. Chen, A. Farshchi, Steric stabilising properties of hydrophobically modified starch: Amylose vs. amylopectin, Food Hydrocoll. 58 (2016) 364–377.
[22] A. Sikorski, Structure of adsorbed polymer chains: a Monte Carlo study, Macromol. Theory Simul. 11 (3) (2002) 359–364.
[23] A. Sikorski, P. Romiszowski, Computer simulations of adsorbed polymer chains, Acta Phys. Pol. B 36 (5) (2005) 1779–1789.
[24] K. Rolińska, A. Sikorski, Adsorption of Linear and Cyclic Multiblock Copolymers from Selective Solvent. A Monte Carlo Study, Macromol. Theory Simul. 29 (6) (2020) 2000053.
[25] M.G. Wessels, A. Jayaraman, Self-assembly of amphiphilic polymers of varying architectures near attractive surfaces, Soft Matter 16 (3) (2020) 623–633.
[26] F.A. Leermakers, F. Léonforte, G.S. Luengo, Structure and Colloidal Stability of Adsorption Layers of Macrocycle Linear, Comb, Star, and Dendritic Macromolecules, Macromolecules 53 (17) (2020) 7322–7334.
[27] P. De Gennes, Polymers at an interface; a simplified view, Adv. Colloid Interface Sci. 27 (3–4) (1987) 189–209.
[28] P. De Gennes, Conformations of polymers attached to an interface, Macromolecules 13 (5) (1980) 1069–1075.
[29] N.L. Green, S.R. Euston, D. Rousseau, Interfacial ordering of tristearin induced by glycerol monooleate and PGPR: A coarse-grained molecular dynamics study, Colloids Surf. B Biointerfaces 179 (2019) 107–113.
[30] A.C. Balazs, C.P. Siemasko, Contrasting the surface adsorption of comb and linear polymers, J. Chem. Phys. 95 (5) (1991) 3798–3803.
[31] C. Van der Linden, F. Leermakers, G.J. Fleer, Adsorption of comb polymers, Macromolecules 29 (3) (1996) 1000–1005.
[32] I. Szleifer, Polymers and proteins: interactions at interfaces, Curr. Opin. Solid State Mater. Sci. 2 (3) (1997) 337–344.
[33] M. Carignano, I. Szleifer, On the structure and pressure of tethered polymer layers in good solvent, Macromolecules 28 (9) (1995) 3197–3204.
[34] F. Felsovalyi, P. Mangiagalli, C. Bureau, S.K. Kumar, S. Banta, Reversibility of the adsorption of lysozyme on silica, Langmuir 27 (19) (2011) 11873–11882.
[35] J. Scheutjens, G.J. Fleer, Statistical theory of the adsorption of interacting chain molecules. 1. Partition function, segment density distribution, and adsorption isotherms, J. Phys. Chem. 83 (12) (1979) 1619–1635.
[36] A. Akinshina, R. Ettelaie, E. Dickinson, G. Smyth, Interactions between adsorbed layers of αS1-casein with covalently bound side chains: a self-consistent field study, Biomacromolecules 9 (11) (2008) 3188–3200.
[37] L. Feuz, F.A. Leermakers, M. Textor, O. Borisov, Adsorption of molecular brushes with polyelectrolyte backbones onto oppositely charged surfaces: A self-consistent field theory, Langmuir 24 (14) (2008) 7232–7244.
[38] R. Israels, F.A. Leermakers, G.J. Fleer, Adsorption of charged block copolymers: effect on colloidal stability, Macromolecules 28 (5) (1995) 1626–1634.
[39] A.A. Polotsky, T. Gillich, O.V. Borisov, F.A. Leermakers, M. Textor, T.M. Birshtein, Dendritic versus Linear Polymer Brushes: Self-Consistent Field Modeling, Scaling Theory, Experiments, Macromolecules 43 (22) (2010) 9555–9566.
[40] F.A. Leermakers, P.J. Atkinson, E. Dickinson, D.S. Horne, Self-Consistent-Field Modeling of Adsorbed beta-Casein: Effects of pH and Ionic Strength on Surface Coverage and Density Profile, J. Colloid Interface Sci. 178 (1996) 681–693.
[41] F.A. Leermakers, M. Ballauff, O.V. Borisov, On the mechanism of uptake of globular proteins by polyelectrolyte brushes- A two-gradient self-consistent field analysis, Langmuir 23 (2007) 3937–3946.

[42] C. Wijmans, J. Scheutjens, E. Zhulina, Self-consistent field theories for polymer brushes: lattice calculations and an asymptotic analytical description, Macromolecules 25 (10) (1992) 2657–2665.
[43] G.J. Fleer, Polymers at interfaces and in colloidal dispersions, Adv. Colloid Interface Sci. 159 (2) (2010) 99–116.
[44] R. Ettelaie, A. Zengin, H. Lee, Fragmented proteins as food emulsion stabilizers: A theoretical study, Biopolymers 101 (9) (2014) 945–958.
[45] I.M. Lifshitz, A.Y. Grosberg, A.R. Khokhlov, Some problems of the statistical physics of polymer chains with volume interaction, Rev. Mod. Phys. 50 (3) (1978) 683–713.
[46] G.J. Fleer, J. Scheutjens, Block copolymer adsorption and stabilization of colloids, Colloids Surf. 51 (1990) 281–298.
[47] R.J. Hunter, Foundations of colloid science, 1, Oxford university press, 1987.
[48] B. Duplantier, Lagrangian tricritical theory of polymer chain solutions near the θ-point, J. Phys. 43 (7) (1982) 991–1019.
[49] A. Johner, Notes on star polymers, EPL (Europhysics Letters) 96 (4) (2011).
[50] A. Striolo, J.M. Prausnitz, Adsorption of branched homopolymers on a solid surface, J. Chem. Phys. 114 (19) (2001) 8565–8572.
[51] G. Kritikos, A.F. Terzis, Adsorption of star polymers studied by a new numerical mean field theory, Polymer 49 (16) (2008) 3601–3609.
[52] S.M. Kilbey, H. Watanabe, M. Tirrell, Structure and Scaling of Polymer Brushes near the ϑ Condition, Macromolecules 34 (15) (2001) 5249–5259.